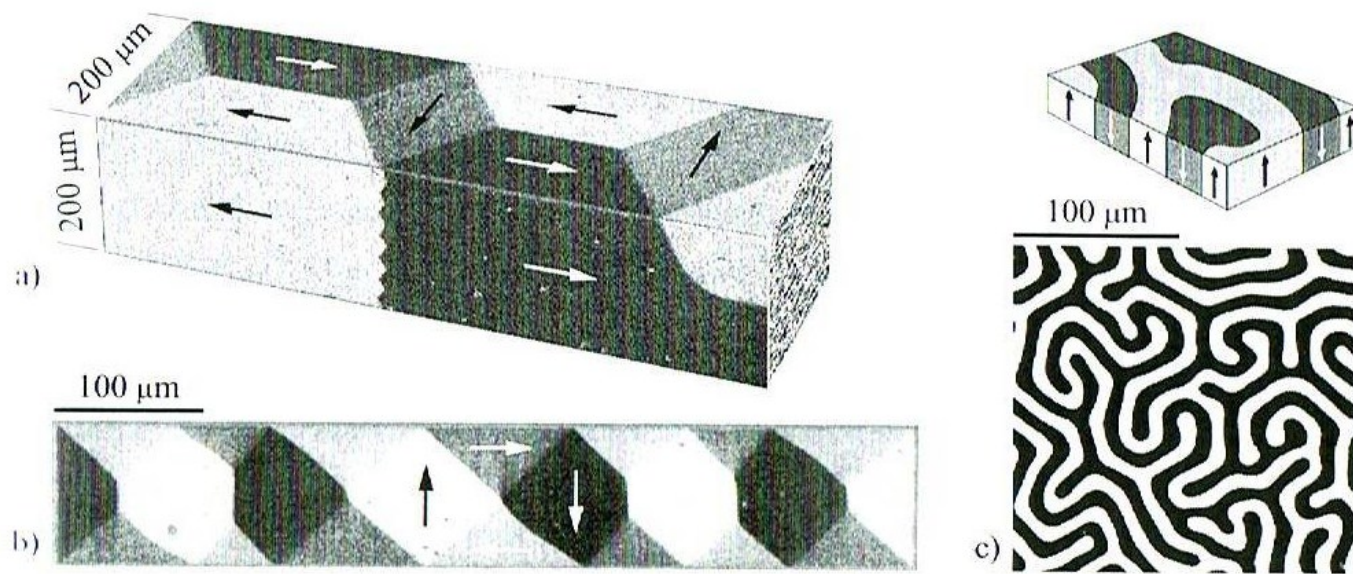
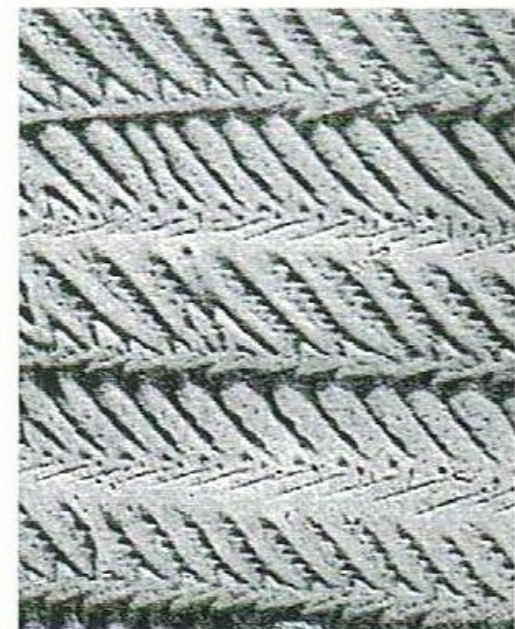


# Magnetic Domains and Domain Walls



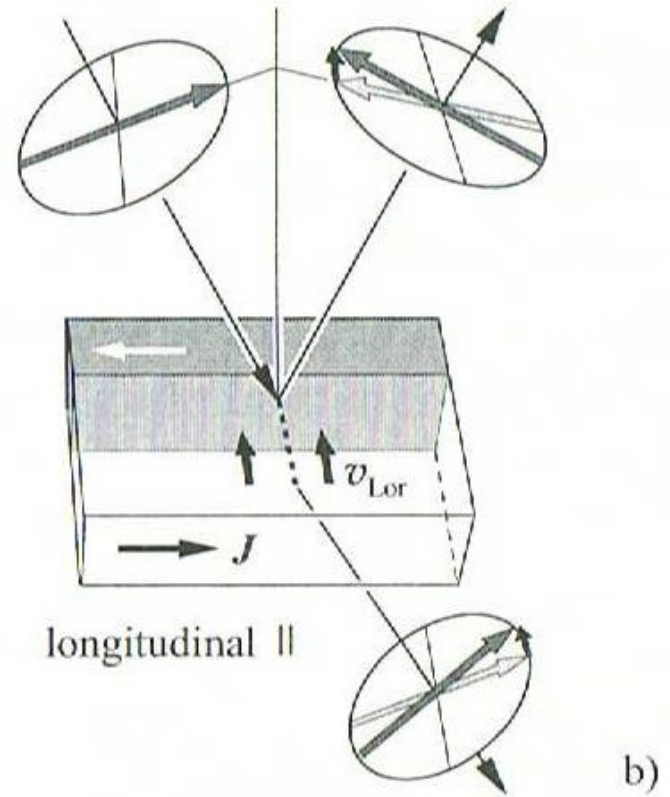
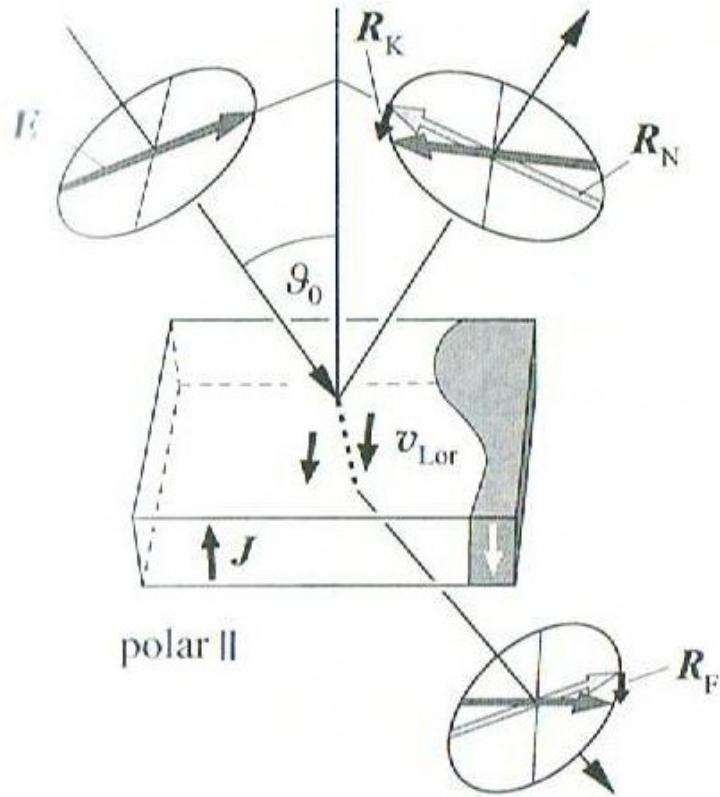
## Bitter-Technique (ferromagnetic colloids on surfaces)



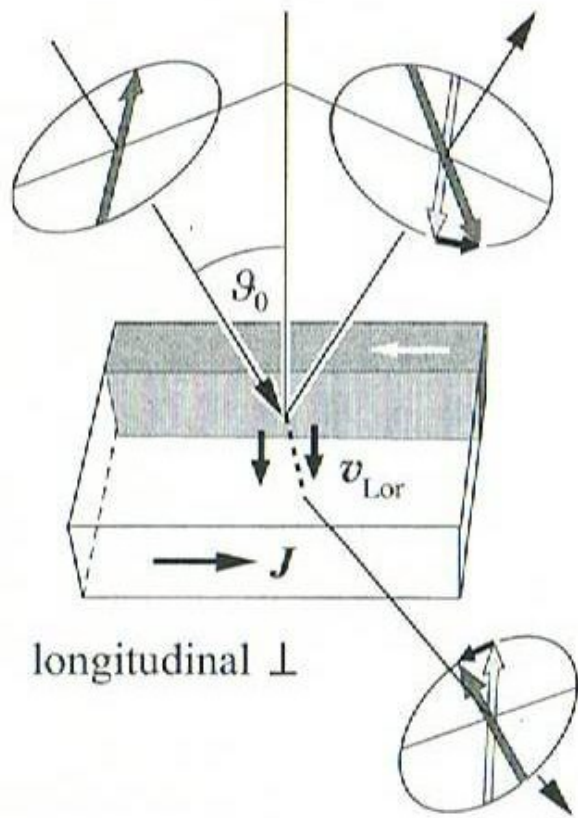
Stress induced domains in NiFe single crystal

# Magneto-optics

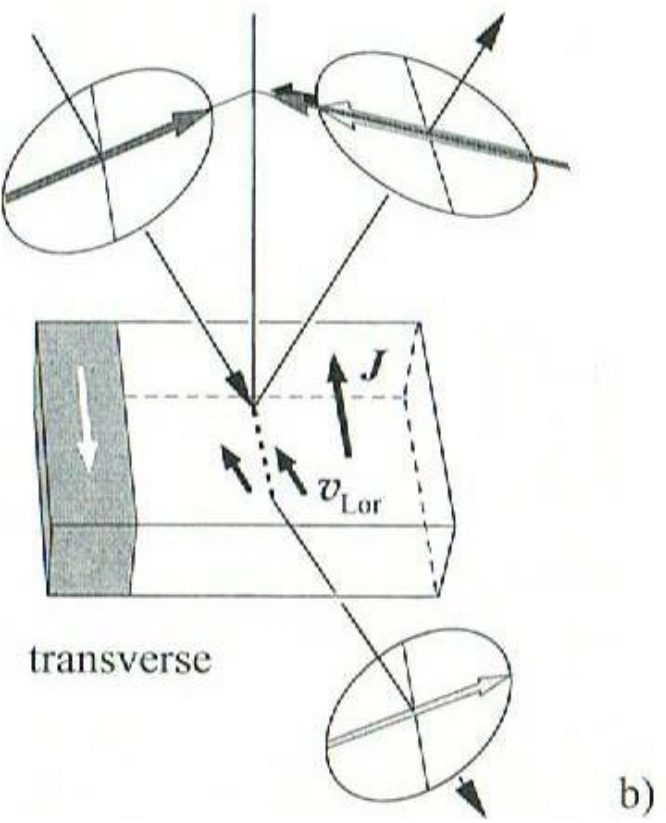
rotations.



Magneto-optical Kerr Effect



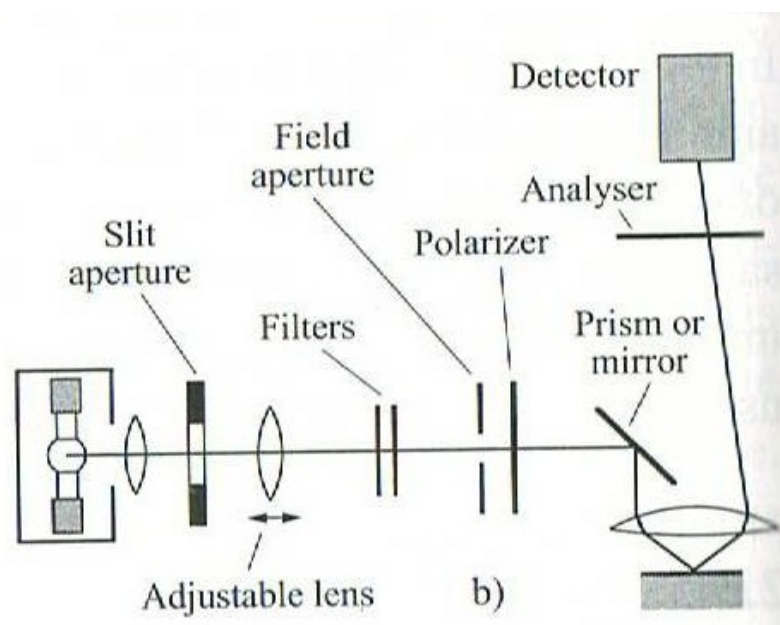
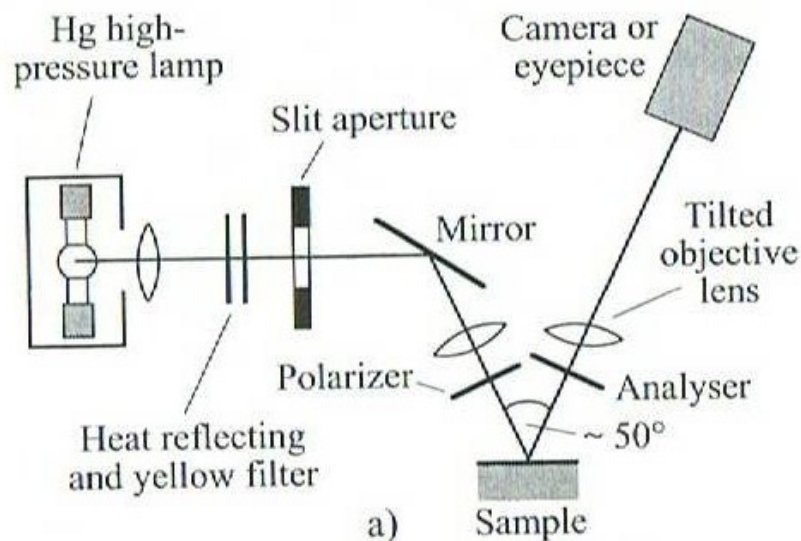
longitudinal  $\perp$

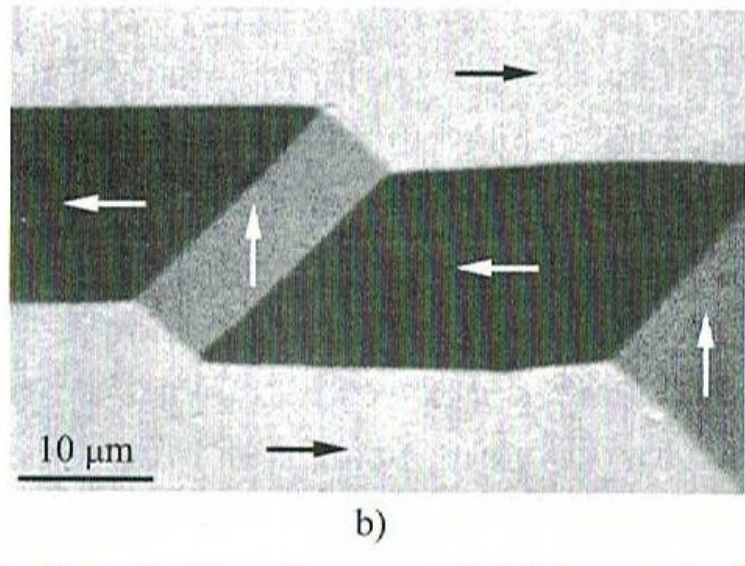
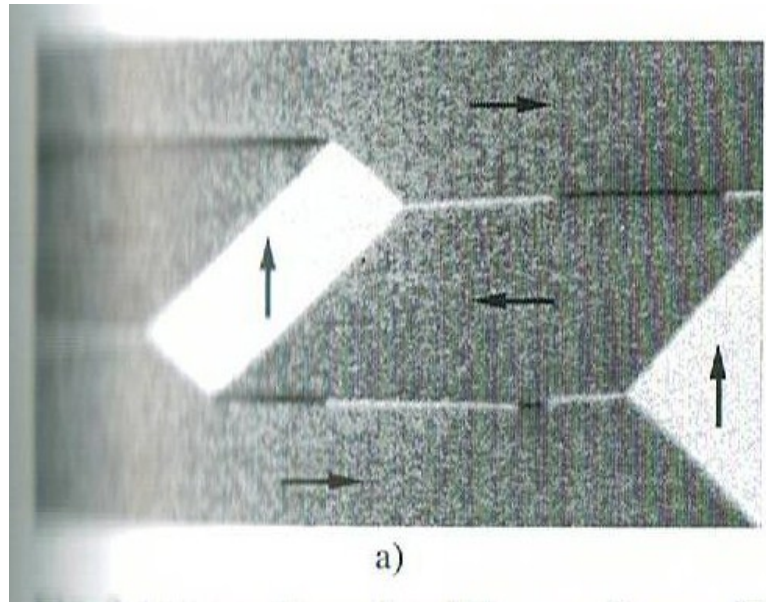


b)

Magneto-optical Kerr Effect

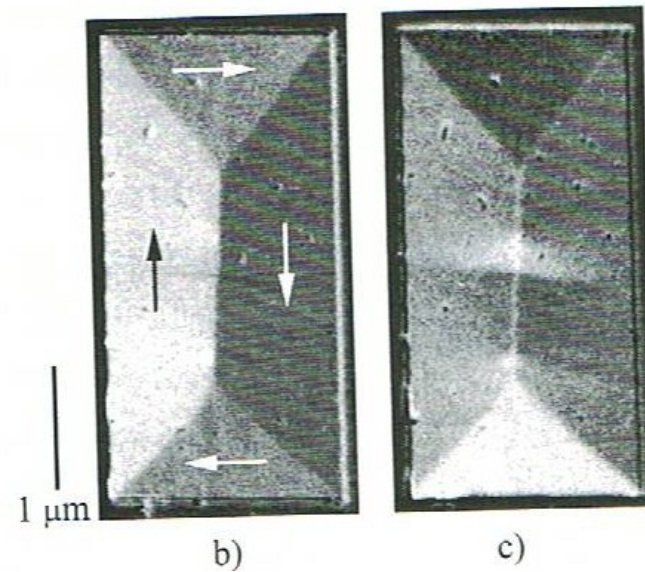
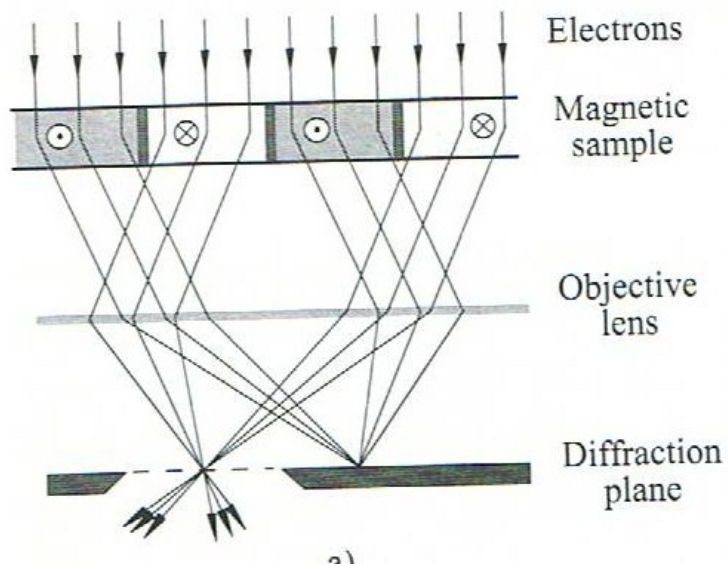
# Kerr microscopes



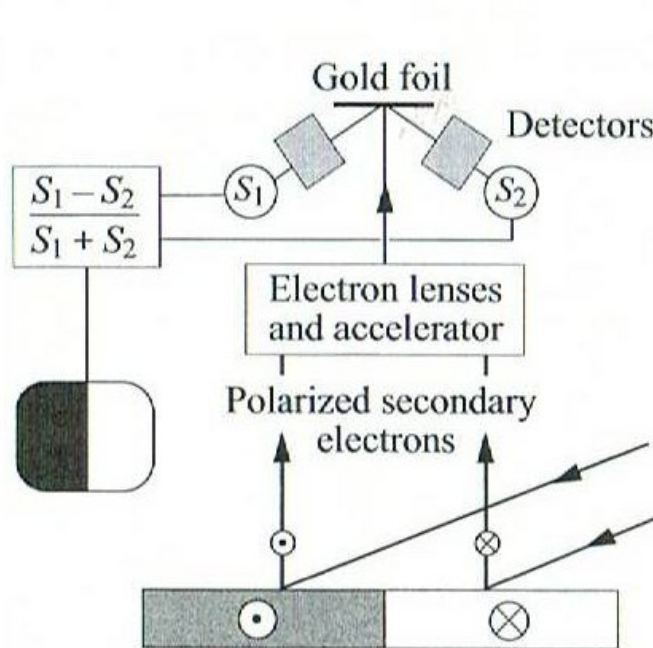


Domains in Fe single crystal

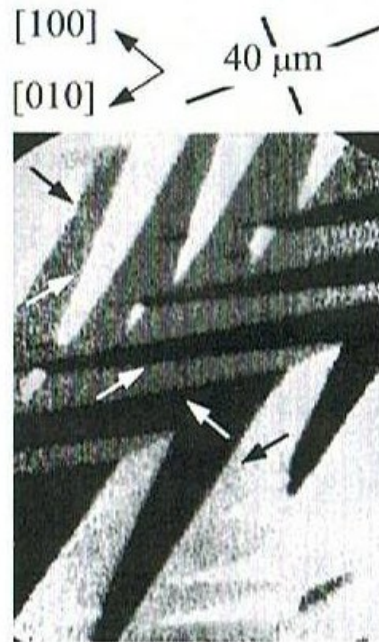
# Transmission electron microscopy Lorentz microscopy



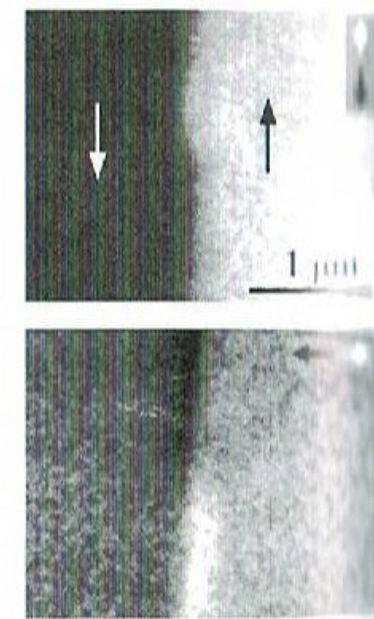
## Scanning electron microscopy with polarization analysis (SEMPA)



a)

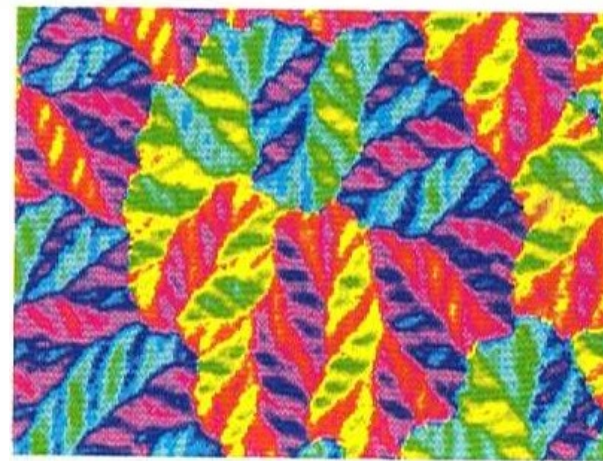


b)

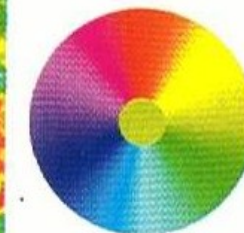


c)

SiFe single crystal



b)



Co single crystal  
(0001)

# Magnetic Force Microscopy

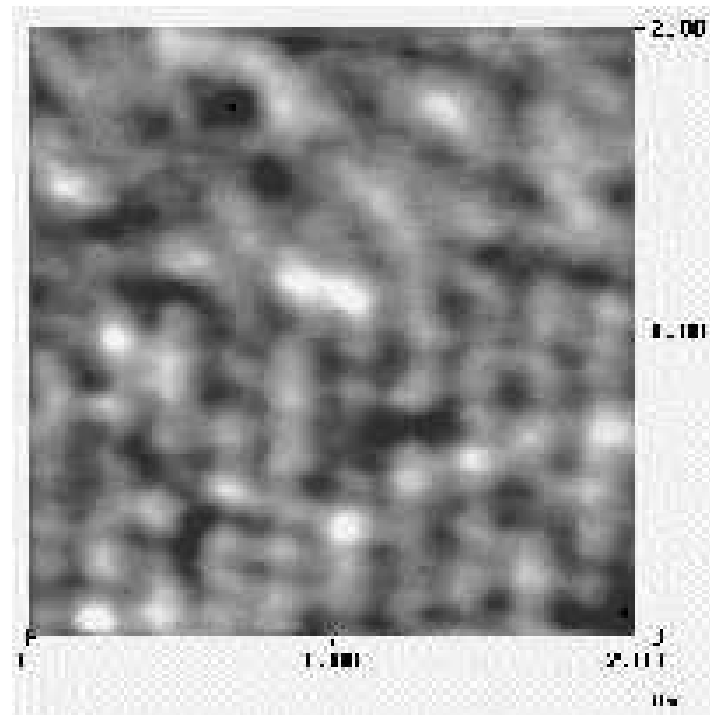
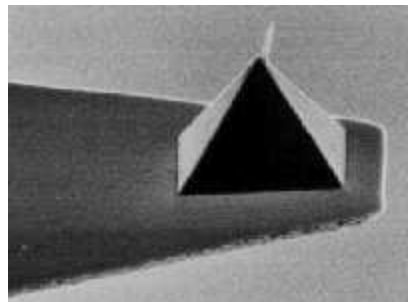
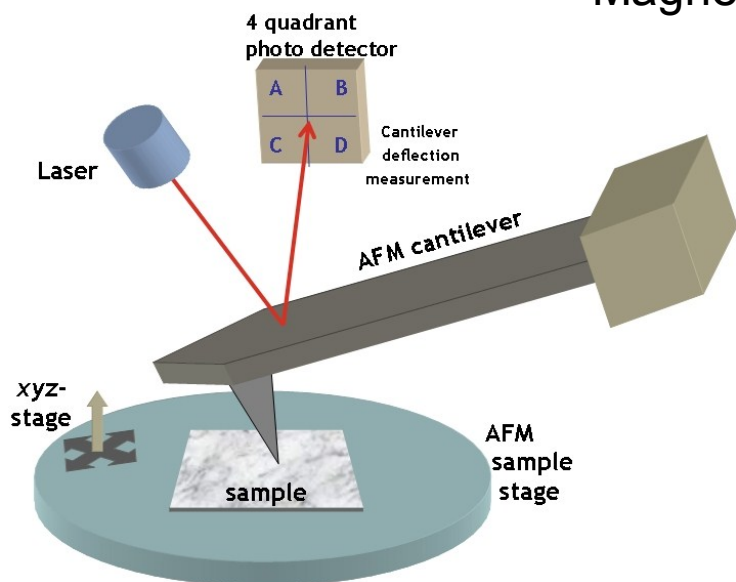
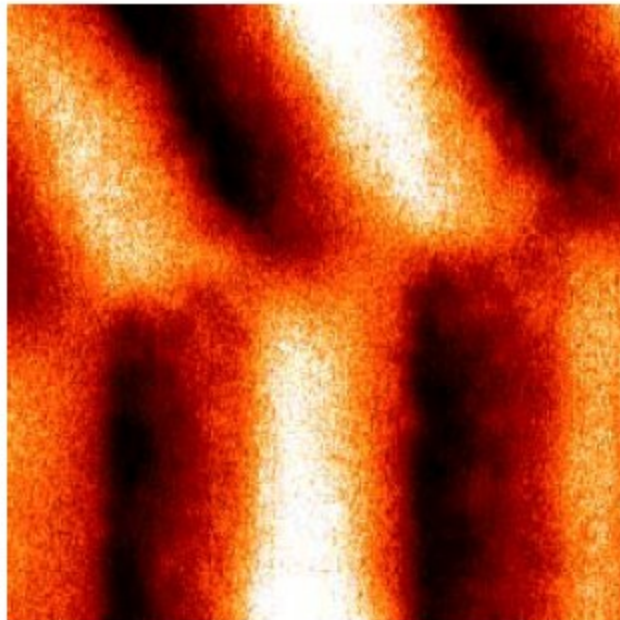
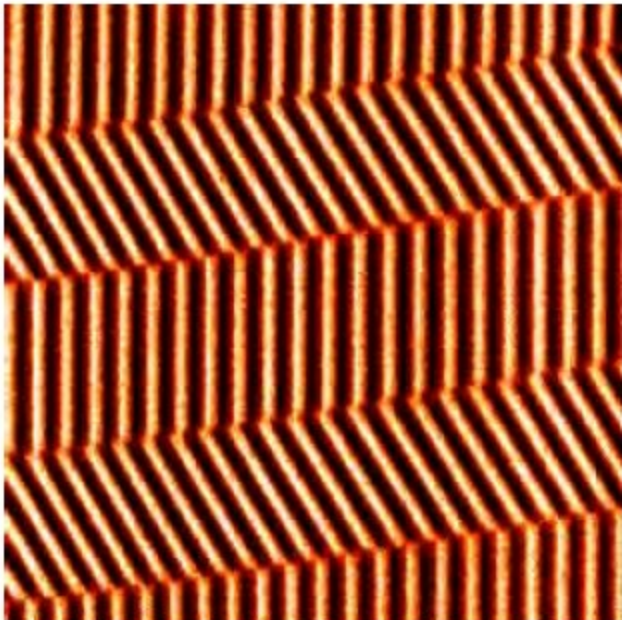
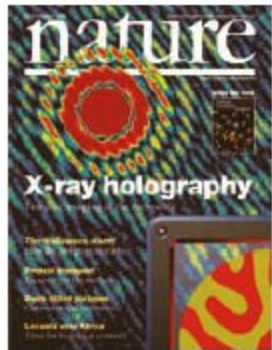


*Image: Border of a 30 µm wide bit track of 300 kfrpi (89 nm bit length)*

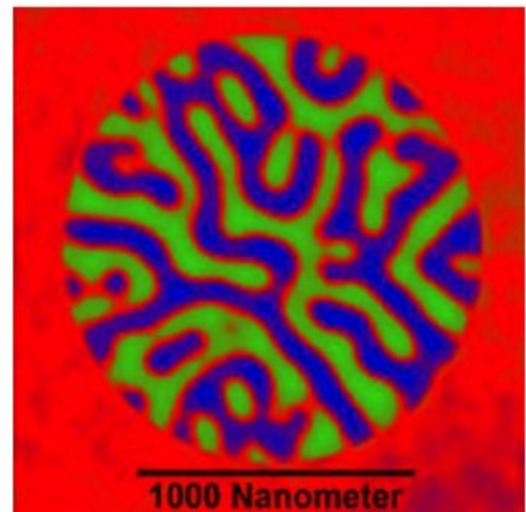
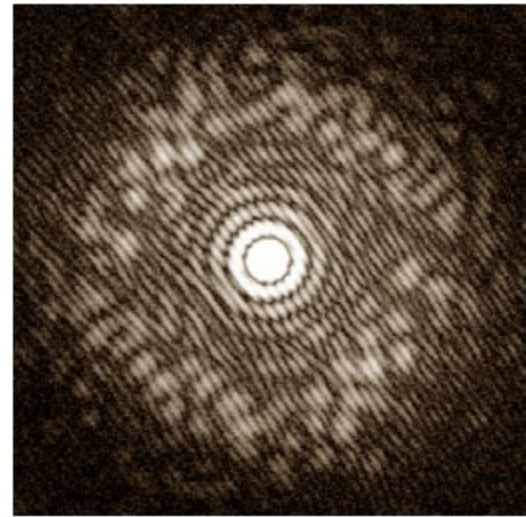
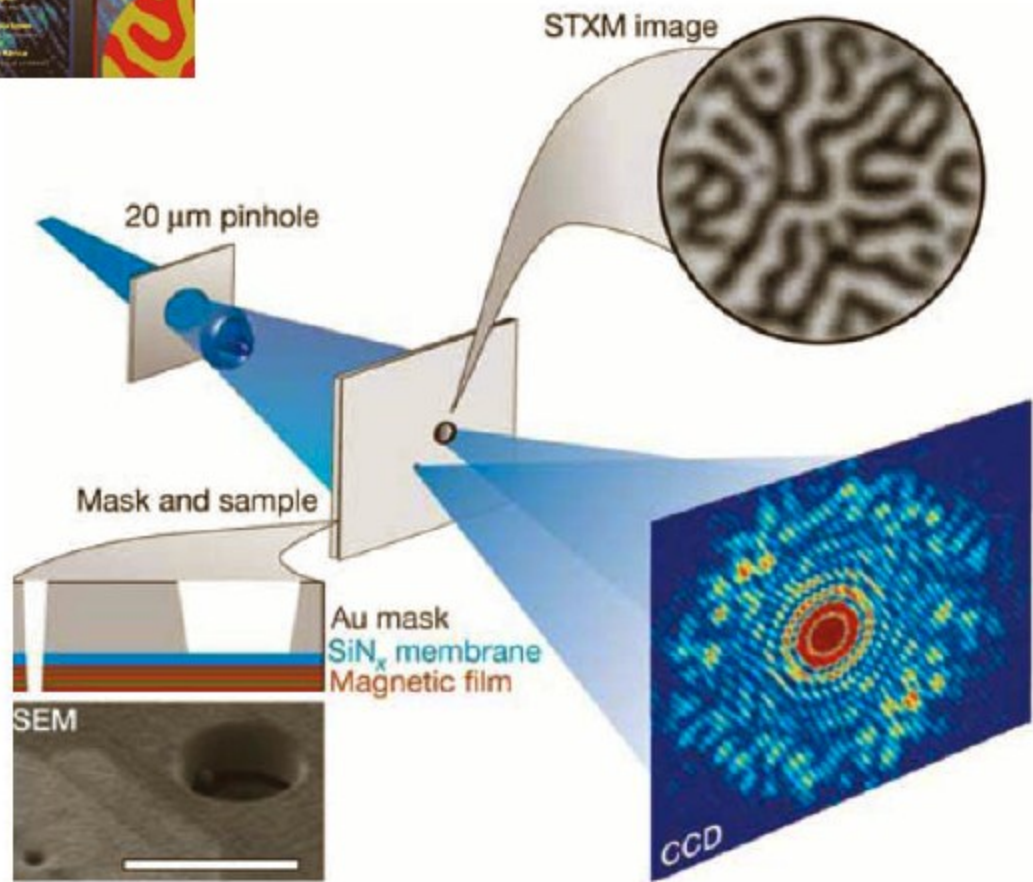
# Magnetic Force Microscopy



Two MFM images of closely spaced bit tracks on a tape, which is used as mass data storage device. While the read head can only distinguish "1" and "0" along the tracks, MFM is able to resolve the fine structure of the magnetic bit structure. Regarding device optimizations the area where neighbouring meet (right image) are of particular importance to increase the bit density.



# XMCD in der Röntgen-Holographie



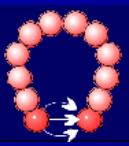
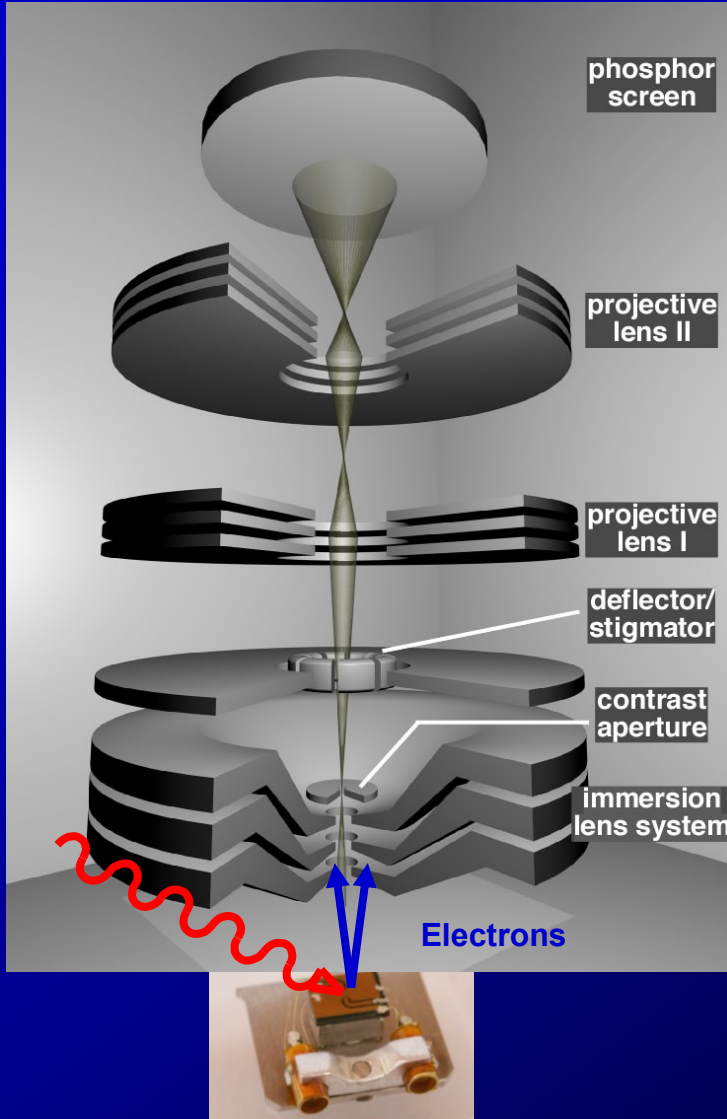
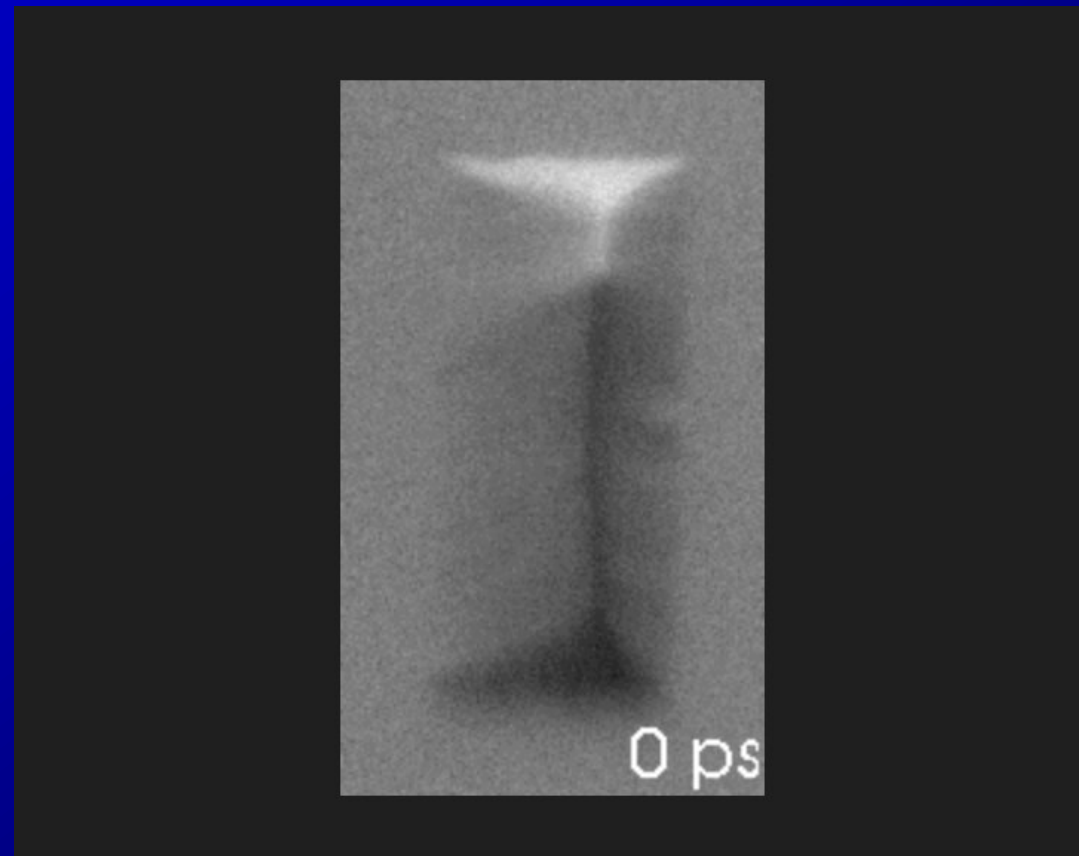
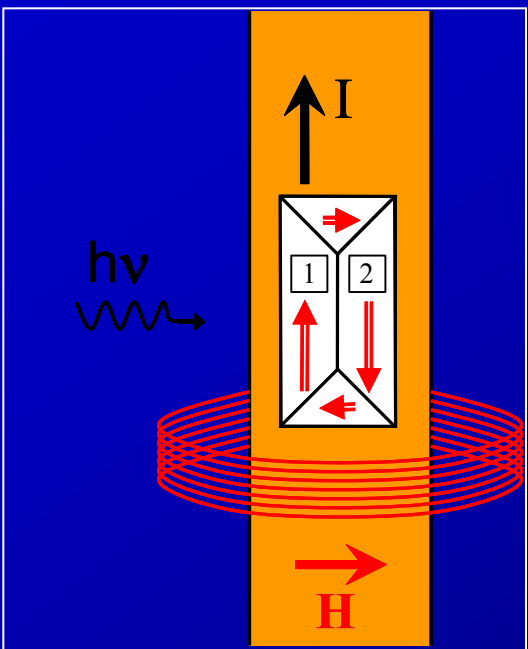


# Photo electron emission microscopy



# Excited oscillation modes

16x32  $\mu\text{m}^2$   
10 nm Py/Cu



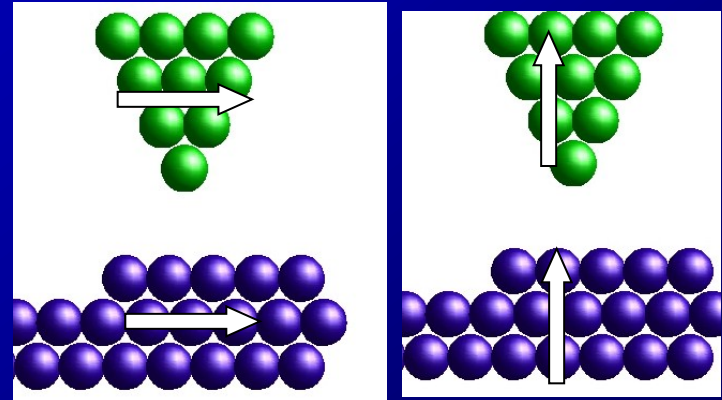
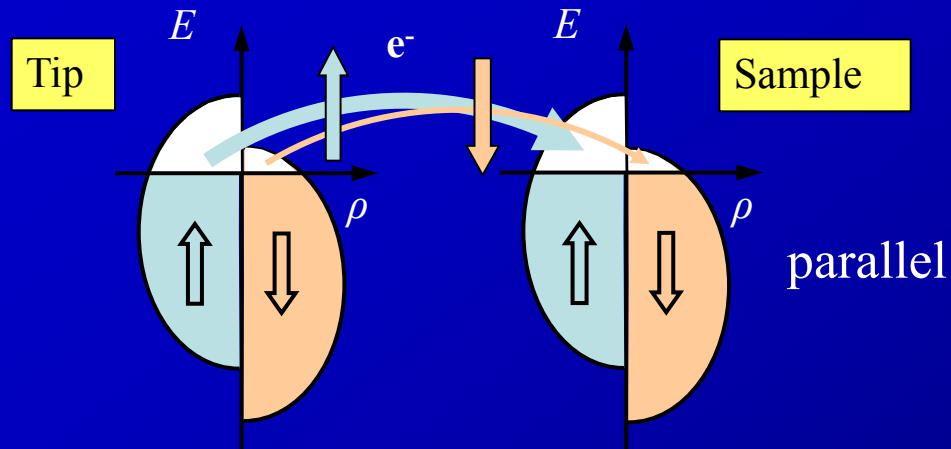
$$A_{\text{XMCD}} \sim \mathbf{M} \cdot \boldsymbol{\sigma} \sim \cos \varphi$$

Oscillating field , 1GHz, 0.2mT

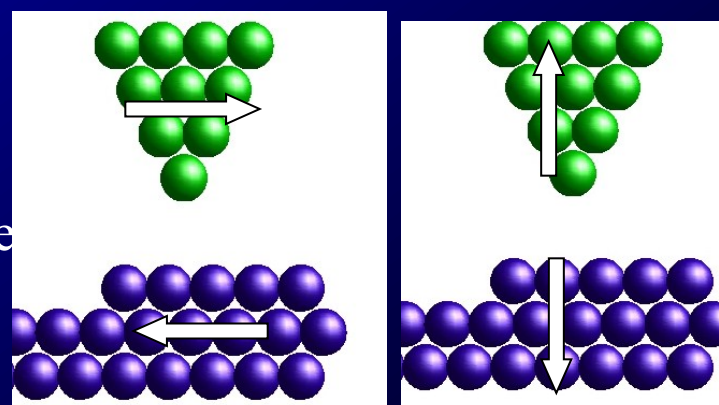
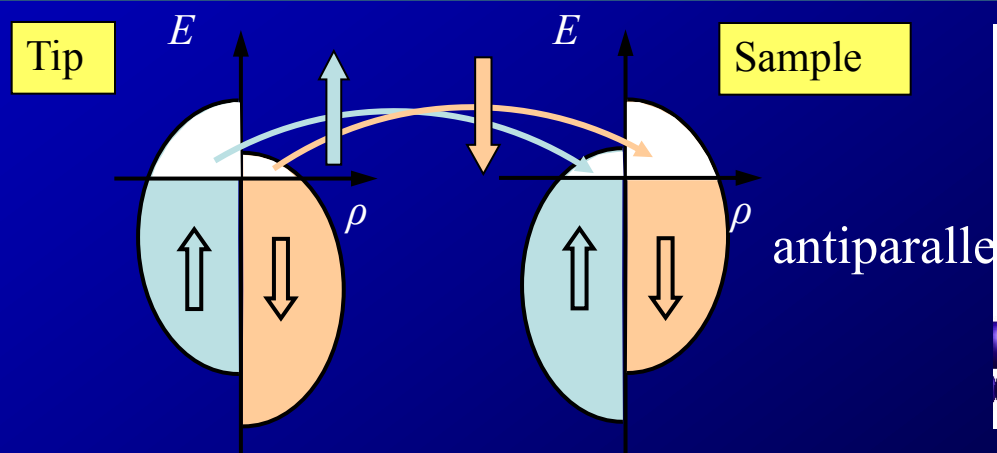
PhD-thesis of A. Krasyuk

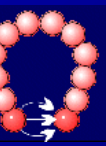


# SP-STM and magnetic contrast



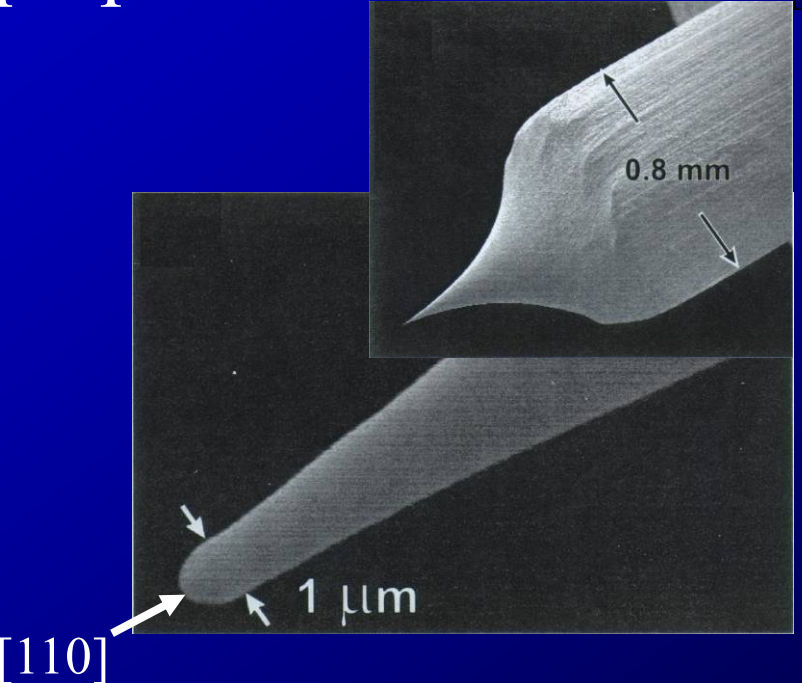
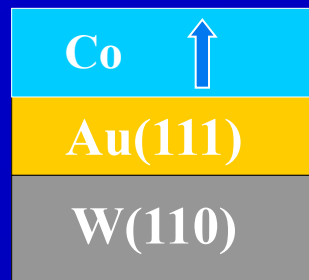
$$\frac{dI}{dU}(U) \propto n_T^{\uparrow}(0)n_S^{\uparrow}(eU) + n_T^{\downarrow}(0)n_S^{\downarrow}(eU) \propto n_T n_S(eU) + m_T m_S(eU) \cdot \cos \angle(\vec{M}_T, \vec{M}_S)$$





# Tip and sample preparation

T. Duden and E. Bauer,  
M. R. S. Proc., 287 (1997).

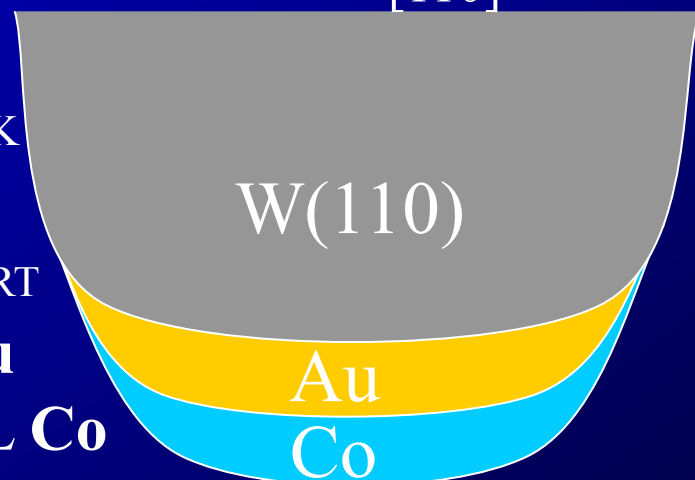


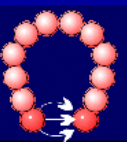
W tips -  
flashing 2000 K

evaporation - RT

10 ML Au

4 – 16 ML Co

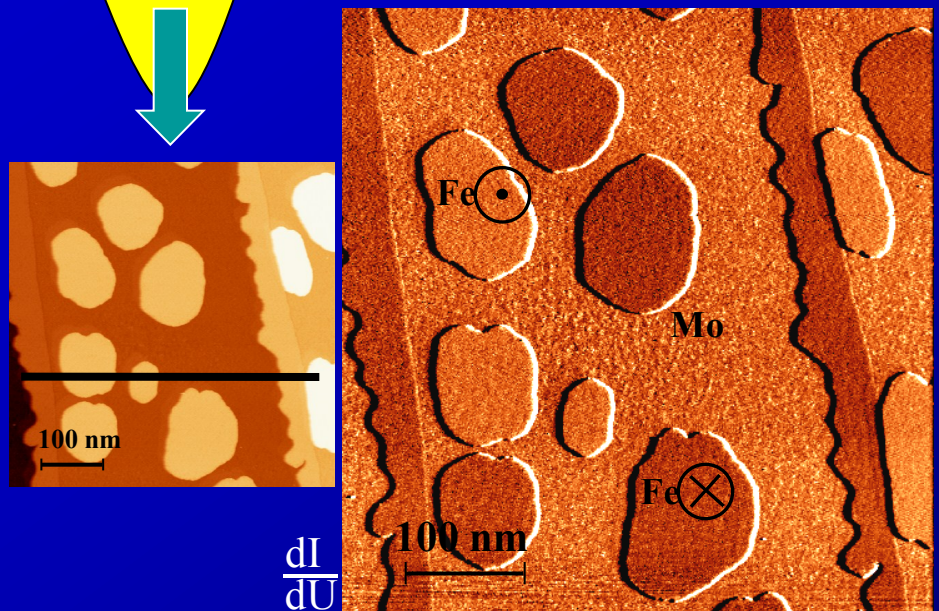




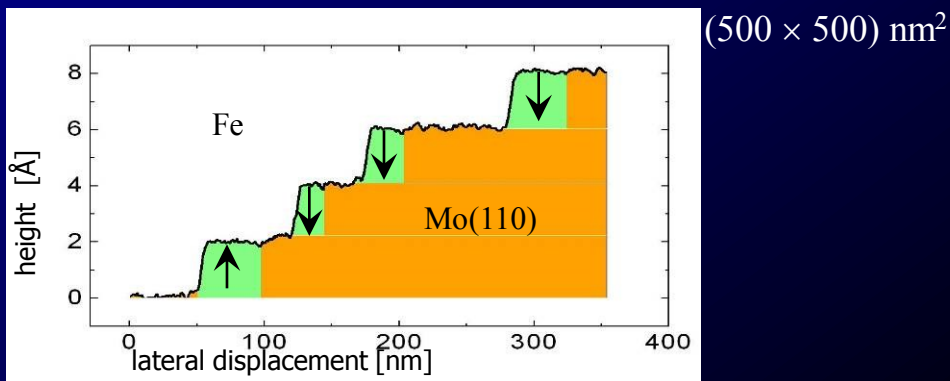
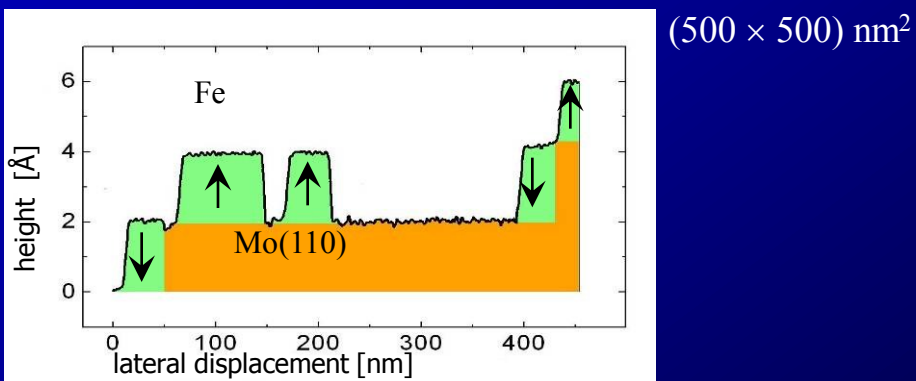
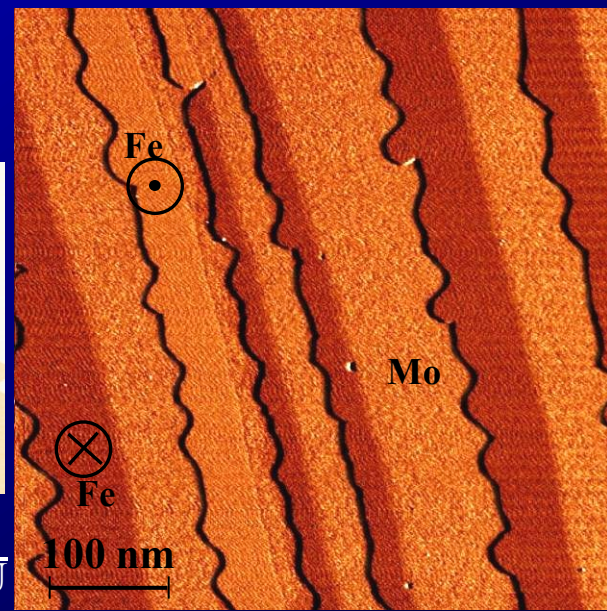
# Out-of-plane magnetic contrast

4 ML Co/Au/W

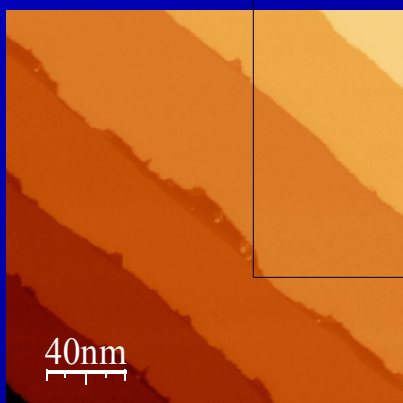
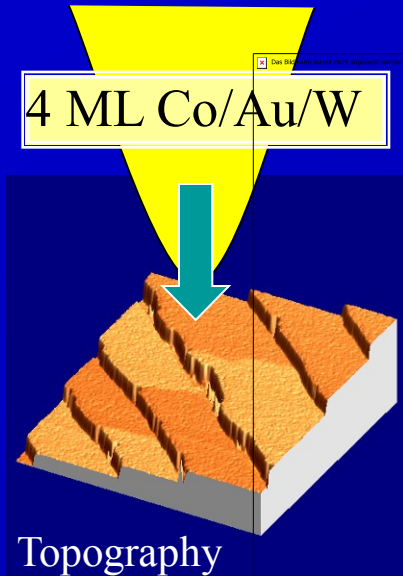
$T = 5\text{ K}$   $I = 1.5\text{ nA}$   $U = 0.3\text{ V}$



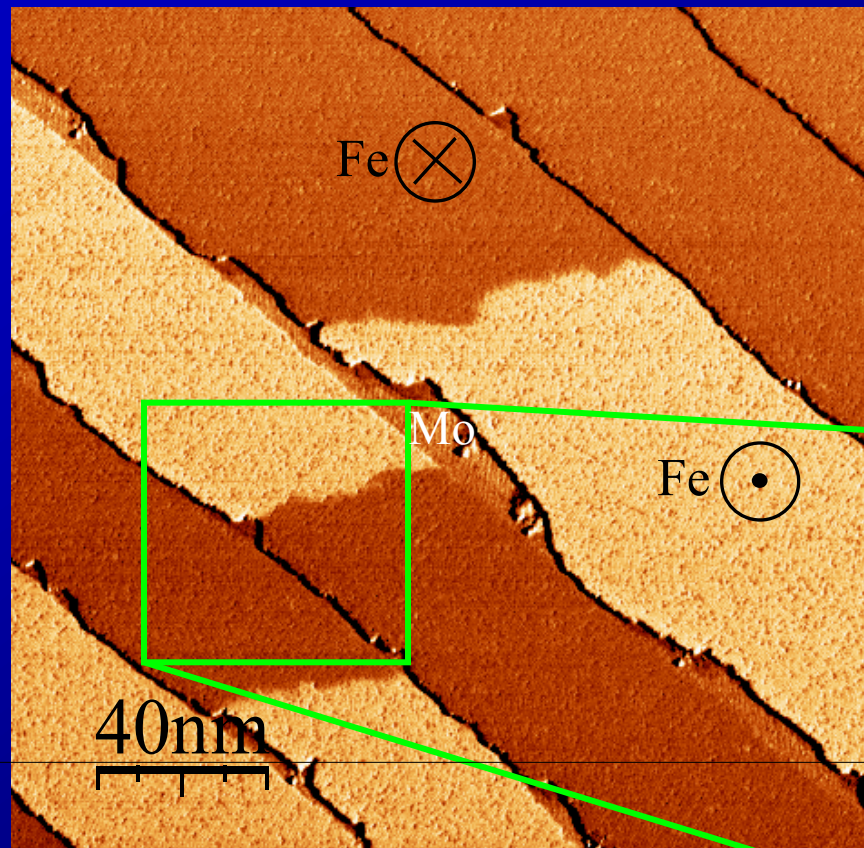
$T = 5\text{ K}$   $I = 1.5\text{ nA}$   $U = 0.4\text{ V}$



# Domain wall width in the ML Fe nanowires

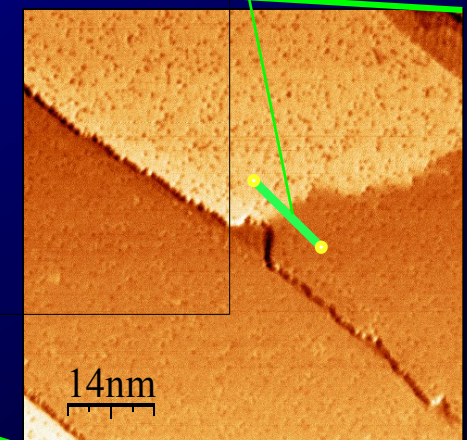
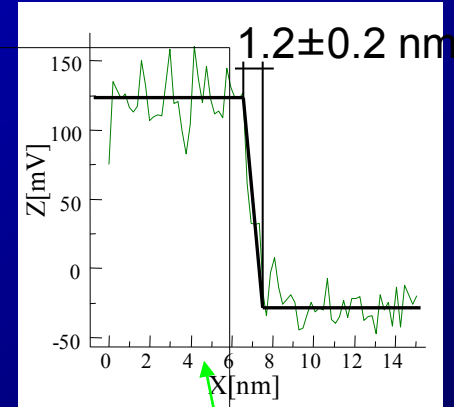


T = 5 K I = 1.5 nA U = 1 V



[001]  
[1̄1̄0]

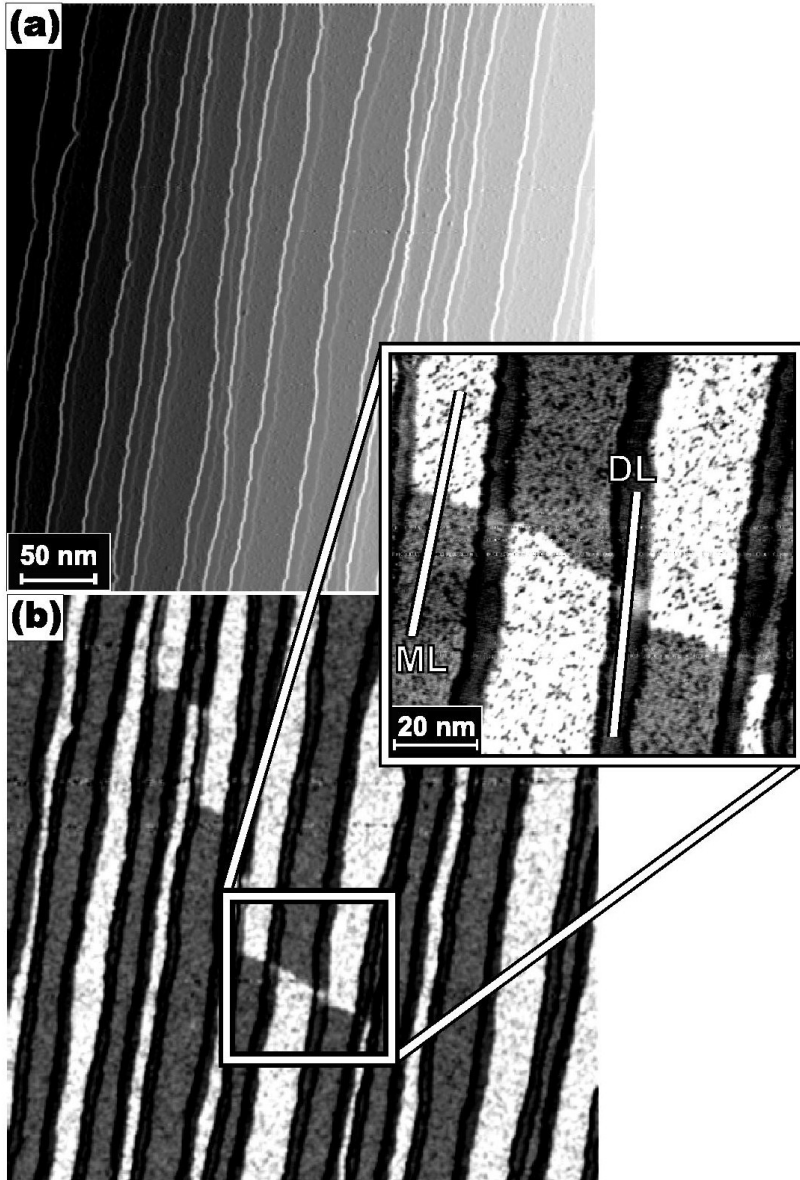
(200 × 200) nm<sup>2</sup>



(70 × 70) nm<sup>2</sup>



# Domain wall width in Fe on W(110)



Domain wall

Width:  $w_{ML} = 6 \text{ \AA}$

Energy:  $e_{ML} = 15.2 \text{ meV/atom row}$

Exchange stiffness

$A = 3.6 \text{ pJ/m (8.2 meV/atom)}$

Anisotropy constant

$K = 41 \text{ MJ/m}^3 (4.0 \text{ meV/atom})$

M. Pratzer, H.J. Elmers, M. Bode, O. Pietzsch,  
A. Kubetzka, and R. Wiesendanger, Phys. Rev.  
Lett. 87, 127201 (2001).

# A. Hubert and R. Schäfer

Springer 1998

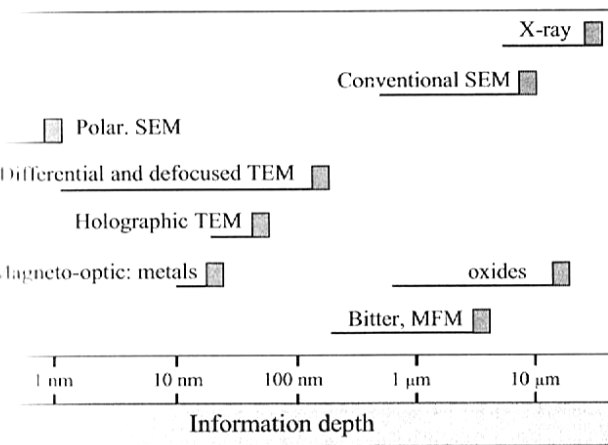
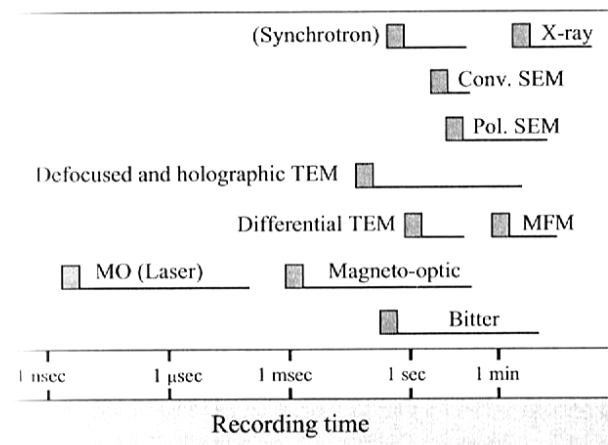
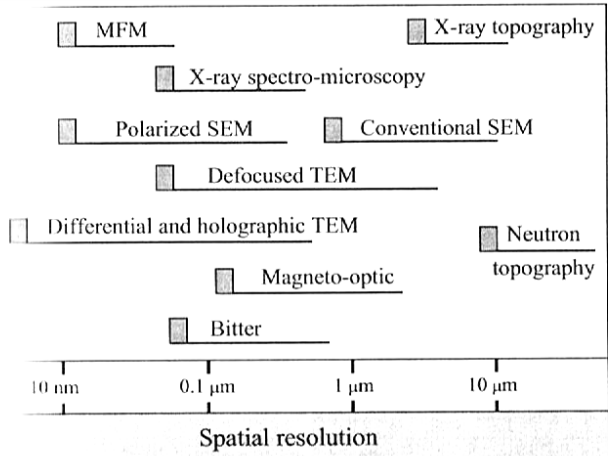


**Fig. 2.56** Comparison of different domain observation techniques. Indicated are the estimated limits of the properties and their approximate range, depending on the experimental conditions